

# Acceleration of Relativistic Protons during the 20 January 2005 Flare and CME

Sophie Masson\*, Karl-Ludwig Klein\*, Rolf Bütikofer<sup>†</sup>, Erwin O. Flückiger<sup>†</sup>,  
Victoria Kurt<sup>‡</sup>, Boris Yushkov<sup>‡</sup>, Säm Krucker<sup>§</sup>

\**Observatoire de Paris, LESIA-CNRS UMR 8109, F-92195 Meudon, France*

<sup>†</sup>*University of Bern, Space Research & Planetary Sciences, CH-3012 Bern, Switzerland*

<sup>‡</sup>*Skobeltsyn Institute of Nuclear Physics, Moscow Lomonossov State University, Moscow 119991, Russia*

<sup>§</sup>*Space Sciences Laboratory, University of California, Berkeley, CA 94720-7450, USA*

**Abstract.** The origin of relativistic solar protons during large flare / CME events has not been uniquely identified so far. We perform a detailed comparative analysis of the time profiles of relativistic protons detected by the worldwide network of neutron monitors at Earth with electromagnetic signatures of particle acceleration in the solar corona during the large particle event of 20 January 2005. The intensity-time profile of the relativistic protons derived from the neutron monitor data indicates two successive peaks. We show that microwave, hard X-ray and  $\gamma$ -ray emissions display several episodes of particle acceleration within the impulsive flare phase. The first relativistic protons detected at Earth are accelerated together with relativistic electrons and with protons that produce pion decay  $\gamma$ -rays during the second episode. The second peak in the relativistic proton profile at Earth is accompanied by new signatures of particle acceleration in the corona within about  $1 R_{\odot}$  above the photosphere, revealed by hard X-ray and microwave emissions of low intensity, and by the renewed radio emission of electron beams and of a coronal shock wave. We discuss the observations in terms of different scenarios of particle acceleration in the corona.

**Keywords:** energetic particles, solar flares, coronal mass ejections

## I. INTRODUCTION

It is still an open question how the Sun accelerates particles, and more specifically, how it can accelerate particles to the relativistic energies which are observed during ground level enhancements (GLE). With flares and coronal shock waves, which both accompany large solar energetic particle (SEP) events (1; 2), solar activity provides candidate environments for particle acceleration. But observations have so far not been able to show unambiguously which of them is the key element for particle acceleration to relativistic energies.

The links of particles detected near 1 AU with their solar origin are blurred by their propagation in interplanetary space, through scattering by the turbulent magnetic field and reflection at large-scale magnetic structures (3; 4; 5; 6). Thus, comparing signatures of accelerated

solar particles at the Sun with the measurements of the relativistic particles at the Earth is often difficult, unless particularly favourable conditions of interplanetary propagation are met. The GLE on 20 January 2005 displays a conspicuous and rapid increase of the relativistic particle flux above the cosmic ray background detected by neutron monitors. The prompt increase and the high anisotropy suggest that the time profiles suffered little distortion by interplanetary scattering. In this paper we report on a detailed timing analysis in a search for common signatures of particle acceleration in GLE time profiles and in electromagnetic emission at the Sun, especially at  $\gamma$ -ray, hard X-ray and radio wavelengths. An extended report is in press (7). A number of other publications has addressed this GLE (8; 9; 10; 11; 12; 13; 14; 15).

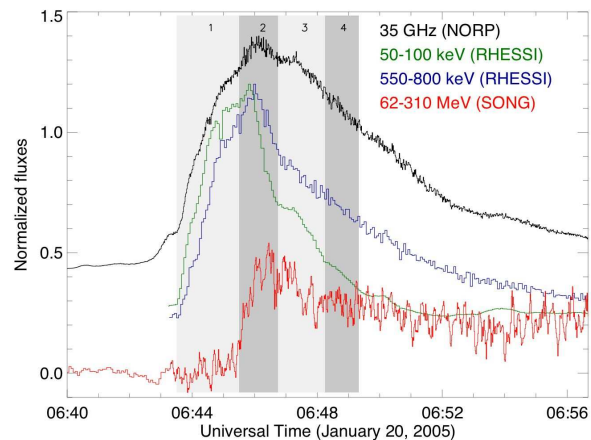


Fig. 1: Time profiles of the normalized flux density at 35 GHz (top) and normalized count rates of hard X-rays and  $\gamma$ -rays (RHESSI, CORONAS-F/SONG) at different energies. Each time profile is normalized by its maximum, and a term is added in order to separate properly the curves. The 35 GHz emission (Nobeyama Radio Polarimeter, courtesy K. Shibasaki) is synchrotron radiation, emissions at (50 – 100) and (550 – 800) keV are bremsstrahlung. The high energy  $\gamma$ -rays are pion decay photons from primary protons at energies above 300 MeV. Different episodes of particle acceleration are distinguished by vertical stripes numbered 1 to 4.

## II. OBSERVATIONS

### A. Particle acceleration in the 20 January 2005 flare

High-energy electrons and protons in the low corona and chromosphere are revealed by their hard X-ray and  $\gamma$ -ray bremsstrahlung, by gyrosynchrotron microwave emission, and different types of nuclear  $\gamma$  radiation. Figure 1 displays the time profiles observed by the Reuven Ramaty High Energy Spectroscopic Imager (RHESSI) (16) in the photon energy ranges 50 – 100 keV (green line) and 550 – 800 keV (blue line), emitted by electrons with energies of order 100 keV and 1 MeV, respectively. The red curve (bottom) shows CORONAS-F/SONG measurements (12) of  $\gamma$ -rays from 62 – 310 MeV. The curve at the top is the microwave time profile at 35 GHz (Nobeyama Radio Polarimeter; 17), emitted by  $\sim 1$  MeV electrons as gyrosynchrotron radiation.

These four time profiles have common structures that reveal distinct episodes of particle acceleration during the flare, with a distinct peak in one or several of these spectral ranges. Four episodes are highlighted in Figure 1 by different tones of grey shading, and are labelled from 1 to 4.

The hard X-ray and microwave emissions start to rise before 06:44 UT (between 06:42 and 06:43 UT at 35 GHz) and display several peaks. The time profile of hard X-rays presents one peak in each of the acceleration phases 1 and 2. The rise to the second peak hides the decrease from the first and vice versa. Both peaks are also seen in the 35 GHz time profile. The initial rise of the hard X-rays is faster, and the first peak is more pronounced, in the 50 – 100 keV range than in the 550 – 800 keV range. Hence relatively more high energy electrons are accelerated during the second acceleration episode than during the first. This reflects the continued spectral hardening throughout most of the event (18).

The appearance of increasingly high particle energies during episode 2 is also reflected by the  $\gamma$ -rays above 60 MeV (Fig. 1, bottom). The count rate starts to rise between 06:43 and 06:45 UT, consistent with an early start of acceleration phase 2, which is hidden in the electron radiation profiles by episode 1. We use as the earliest time the start of the high-energy  $\gamma$ -ray emission at 06:45:30 UT. The count rate is dominated by pion decay emission, as shown in (7).

We conclude from these time profiles that high energy electrons and protons were accelerated in the corona during the impulsive phase of the event, but that the impulsive phase itself was structured into different acceleration episodes lasting about 1 min each. The most energetic particles were not accelerated since the start of the events, but during the second acceleration episode identified in the time profiles, three to four minutes after the first signatures of electron acceleration.

Imaging observations of this event at hard X-rays and  $\gamma$ -rays (19) show the usual configuration of bright chromospheric footpoints of coronal loops, on top of UV ribbons, together with a presumably coronal  $\gamma$ -

ray source. Such observations are commonly ascribed to a complex magnetic topology implying magnetic reconnection in the low corona.

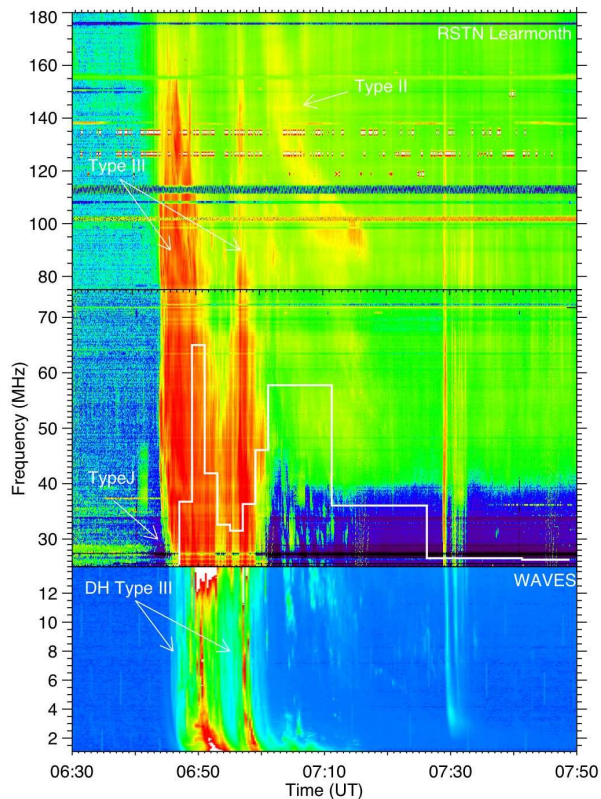


Fig. 2: Dynamic spectrum of the metric-to-decametric radio emission during the 20 January 2005 event, observed at the Learmonth station of the RSTN network (180 – 25 MHz) and the *Wind*/WAVES spectrograph (14 – 1 MHz). The overplotted white curve is the time history of the proton intensity at 5 GV rigidity (kinetic energy 4.15 GeV), shifted backward by 216 s.

### B. Particle confinement and escape in the 20 January 2005 flare inferred from radio observations

Metric-to-hectometric radio emissions of non-thermal electrons from the middle corona to the interplanetary medium are measured respectively by the RSTN network<sup>1</sup> (25 – 180 MHz; we use data from the Learmonth station) and the *Wind*/WAVES experiment in the range 0.04-14 MHz (20). The combined spectrum of the two instruments in the 1 – 180 MHz band, corresponding roughly to a range of heliocentric distances between 1.2 and 10 – 20  $R_{\odot}$ , is represented in Fig. 2. Different burst groups can be distinguished.

The emission below 14 MHz starts with two bright type III burst groups (06:45 to 06:55 UT and 06:57 to 07:00 UT), which extend up to metre waves. This emission is produced by electron beams near the electron plasma frequency or its harmonic. The starting frequency

<sup>1</sup><http://www.ngdc.noaa.gov/stp/SOLAR/ftpsolarradio.html#spectralgraphs>

is above the RSTN high-frequency limit of 180 MHz, which means the electron beams started in the low corona, where the ambient density exceeds  $10^8 \text{ cm}^{-3}$ . Closer inspection of the spectra shows that the first metre wave burst in the RSTN spectrum bends around to form a type J burst between 35 and 25 MHz. Hence electrons accelerated during the first acceleration episode (Fig. 1) do not seem to get access to interplanetary space, but propagate in closed coronal magnetic structures.

Thus, we conclude that the first injection of electron beams into interplanetary space is traced by the first faint DH type III burst (frequency  $\leq 14$  MHz) at 06:45 UT  $\pm 30$  s, and is followed by a series of more intense injections corresponding to the first bright DH type III group. This means that the first high energy electrons and protons, which were accelerated during the second acceleration episode, got immediate access to the high corona and interplanetary space through open magnetic flux tubes.

### C. The relationship with the GLE

This picture is consistent with the timing of the GLE. The rigidity spectrum and the angular distribution of relativistic protons was derived from the analysis of 40 neutron monitors of the worldwide network (15; 7). The time profiles of the type III emission at 14 MHz and of the proton intensity at 5 GV, which corresponds to a kinetic energy of 4.15 GeV, display similarly rapid initial rise phases and, broadly speaking, two peaks. These similarities suggest a common release of the relativistic protons and the radio emitting electron beams. The initial rise phases coincide when the proton profile is shifted backward by  $t_{\text{shift}} = 216$  seconds. This backward shifted proton profile is overplotted by the white line on the radio spectrum in Fig. 2.

The delay of 216 s gives only a lower limit of the travel time, because the acceleration region is presumably much closer to the Sun than the 14 MHz source. We determine the upper limit of the path length, assuming that the first escaping relativistic protons were accelerated with the protons that created pions in the low solar atmosphere. This implies a supplementary travel time of the protons with respect to photons of 4.5 min. Given the velocity of  $0.98c$  of 5 GV protons and the light travel time of 489 s from Sun to Earth on this day, the delay of 4.5 min implies that the protons travelled a distance of about 1.5 AU in interplanetary space.

We conclude that the  $\gamma$ -ray emission, the confinement and escape of particles inferred from radio observations, and the GLE timing observed by neutron monitors are consistent with the common acceleration and release of the flare-related radiating protons and the relativistic protons during the first peak of the GLE.

### D. The second peak of the GLE

The time profile of the proton intensity shows a second peak that lasts longer than the first. Provided the path length of the relativistic protons is the same

as during the first peak, the onset of this second peak coincides with the second group of type III bursts seen from 1 to 180 MHz, and the entire peak of the peak is accompanied by the type II burst between 75 and 180 MHz, which is generally interpreted as radio emission from a shock wave propagating through the corona. If it is harmonic plasma emission, the ambient electron densities in the metric type II source range from  $10^8$  to  $2 \times 10^7 \text{ cm}^{-3}$ .

The type III and type II bursts occur on top of a diffuse background (green in Fig. 2) that reveals gyrosynchrotron emission from mildly relativistic electrons. It starts together with the first metric type III bursts and continues throughout the plotted time interval. It can be identified until at least 07:50 UT in single frequency records, with broadband fluctuations from centimetre to metre waves that suggest repeated electron injection.

The start of the second peak of relativistic protons is associated with a new, short group of type III bursts and a faint rise of the decaying microwave and hard X-ray time profiles. This implies a renewed acceleration, similar to the previous impulsive phase, which might also accelerate relativistic protons. The bulk of the proton peak accompanies the metric type II burst, which may suggest shock acceleration of the second peak (see also 14). But, as noted by (21), the shock wave is not the bow shock of the CME observed by LASCO/SOHO, whose front is near heliocentric distance of  $4.5 R_{\odot}$  when the type II burst starts. This distance is inconsistent with metre wave type II emission, which suggests a source within  $2 R_{\odot}$  from the Sun's centre. The exciter of the type II burst is also much slower than the CME front: the measured relative frequency drift rate is  $-6.8 \times 10^{-4} \text{ s}^{-1}$ . Such a drift is produced by an exciter that moves at a speed of roughly  $500 \text{ km s}^{-1}$  along a hydrostatic density gradient (electron-proton plasma,  $T = 1.5 \times 10^6 \text{ K}$ ) at heliocentric distance  $2 R_{\odot}$ . This is much lower than the speed of the CME, which was estimated between 2000 and  $2600 \text{ km s}^{-1}$  (13). If the second peak in the relativistic proton profile is due to shock acceleration, it must be accelerated at the flanks of the CME, not at its front.

## III. CONCLUSION

The 20 January 2005 GLE displays two peaks in the relativistic proton profile. The first is closely related in time to the acceleration of high energy particles in the flare, and their escape to interplanetary space. The second could also be related with particle acceleration in the corona, and possibly with a shock. GLE scenarios including two components, called a prompt one and a delayed one, had been introduced before (22; 23). The delayed component was ascribed to acceleration at a CME-driven shock wave. While the present analysis is consistent with this two-component injection, it also shows that the coronal acceleration history is much more complex: there is no unique flare-related acceleration, but the impulsive flare phase is itself structured, as has

long been known from hard X-ray observations (24). If a coronal shock wave accelerates relativistic protons in a later phase of the event, it is not necessarily the bow shock of the CME which is the key element. Clearly, detailed comparative timing analyses of GLEs and flare/CME tracers provide relevant constraints to understand the origin of relativistic particles at the Sun.

#### REFERENCES

- [1] H. V. Cane, W. C. Erickson, and N. P. Prestage, “Solar flares, type III radio bursts, coronal mass ejections and energetic particles,” *JGR*, vol. 107, p. 1315 (doi:10.1029/2001JA000320), 2002.
- [2] N. Gopalswamy, S. Yashiro, S. Krucker, G. Stenborg, and R. A. Howard, “Intensity variation of large solar energetic particle events associated with coronal mass ejections,” *JGR*, vol. 109, p. A12105 (doi: 10.1029/2004JA01602), 2004.
- [3] P. Meyer, E. N. Parker, and J. A. Simpson, “Solar cosmic rays of February, 1956 and their propagation through interplanetary space,” *Physical Review*, vol. 104, pp. 768–783, Nov. 1956.
- [4] W. Dröge, “Particle scattering by magnetic fields,” *Space Sci. Rev.*, vol. 93, pp. 121–151, 2000.
- [5] J. W. Bieber, W. Dröge, P. A. Evenson et al., “Energetic particle observations during the 2000 July 14 solar event,” *ApJ*, vol. 567, pp. 622–634, Mar. 2002.
- [6] A. Sáiz, D. Ruffolo, J. W. Bieber, P. Evenson, and R. Pyle, “Anisotropy signatures of solar energetic particle transport in a closed interplanetary magnetic loop,” *ApJ*, vol. 672, pp. 650–658, Jan. 2008.
- [7] S. Masson, K.-L. Klein, R. Bütikofer et al., “Acceleration of relativistic protons during the 20 January 2005 flare and CME,” *Solar Phys.*, *in press*, 2009.
- [8] J. Bieber, J. Clem, P. Evenson, et al., “Largest GLE in half a century : neutron monitor observations of the January 20, 2005 event,” in *29th International Cosmic Ray Conference*, vol. 1, 2005, pp. 237–240.
- [9] G. M. Simnett, “The timing of relativistic proton acceleration in the 20 January 2005 flare,” *A&A*, vol. 445, pp. 715–724, 2006.
- [10] C. Plainaki, A. Belov, E. Eroshenko, H. Mavromichalaki, and V. Yanke, “Modeling ground level enhancements: Event of 20 January 2005,” *JGR*, vol. 112, p. 4102, Apr. 2007.
- [11] D. J. Bombardieri, M. L. Duldig, J. E. Humble, and K. J. Michael, “An improved model for relativistic solar proton acceleration applied to the 2005 January 20 and earlier events,” *ApJ*, vol. 682, pp. 1315–1327, Aug. 2008.
- [12] S. N. Kuznetsov, V. G. Kurt, B. Y. Yushkov, and K. Kudela, “CORONAS-F satellite data on the delay between the proton acceleration on the Sun and their detection at 1 AU,” in *30th International Cosmic Ray Conference*, R. Caballero, J. C. D’Olivo, G. Medina-Tanco, L. Nellen, F. A. Sánchez, and J. F. Valdés-Galicia, Eds., vol. 1, 2008, pp. 121–124.
- [13] V. V. Grechnev, V. G. Kurt, I. M. Chertok, et al., “An Extreme Solar Event of 20 January 2005: Properties of the Flare and the Origin of Energetic Particles,” *Solar Phys.*, vol. 252, pp. 149–177, Oct. 2008.
- [14] K. G. McCracken, H. Moraal, and P. H. Stoker, “Investigation of the multiple-component structure of the 20 January 2005 cosmic ray ground level enhancement,” *JGR*, vol. 113, p. 12101, Dec. 2008.
- [15] R. Bütikofer, E. O. Flückiger, L. Desorgher, M. R. Moser, and B. Pirard, “The solar cosmic ray ground-level enhancements on 20 January 2005 and 13 December 2006,” *Adv. Space Res.*, vol. 43, pp. 499–503, Feb. 2009.
- [16] R. P. Lin, B. R. Dennis, G. J. Hurford et al., “The Reuven Ramaty High-Energy Solar Spectroscopic Imager (RHESSI),” *Solar Phys.*, vol. 210, pp. 3–32, Nov. 2002.
- [17] H. Nakajima, H. Sekiguchi, M. Sawa, K. Kai, and S. Kawashima, “The radiometer and polarimeters at 80, 35, and 17 GHz for solar observations at Nobeyama,” *PASJ*, vol. 37, pp. 163–170, 1985.
- [18] R. Saldanha, S. Krucker, and R. P. Lin, “Hard X-ray spectral evolution and production of solar energetic particle events during the January 2005 X-class flares,” *ApJ*, vol. 673, pp. 1169–1173, Feb. 2008.
- [19] S. Krucker, G. J. Hurford, A. L. MacKinnon, A. Y. Shih, and R. P. Lin, “Coronal  $\gamma$ -ray bremsstrahlung from solar flare-accelerated electrons,” *ApJ*, vol. 678, pp. L63–L66, May 2008.
- [20] J.-L. Bougeret, M. L. Kaiser, P. J. Kellogg et al., “Waves: The Radio and Plasma Wave Investigation on the Wind Spacecraft,” *Space Sci. Rev.*, vol. 71, pp. 231–263, 1995.
- [21] S. Pohjolainen, L. van Driel-Gesztelyi, J. L. Culhane, P. K. Manoharan, and H. A. Elliott, “CME propagation characteristics from radio observations,” *Solar Phys.*, vol. 244, pp. 167–188, Aug. 2007.
- [22] J. Torsti, L. G. Kocharov, R. Vainio, A. Anttila, and G. A. Kovaltsov, “The 1990 May 24 solar cosmic-ray event,” *Solar Phys.*, vol. 166, pp. 135–158, Jun. 1996.
- [23] L. I. Miroshnichenko, C. A. De Koning, and R. Perez-Enriquez, “Large solar event of September 29, 1989: ten years after,” *Space Sci. Rev.*, vol. 91, pp. 615–715, 2000.
- [24] C. de Jager and G. de Jonge, “Properties of elementary flare bursts,” *Solar Phys.*, vol. 58, pp. 127–137, Jun. 1978.